ARTICLES

Investigation of nuclear charge symmetry by pion elastic scattering from ^{3}H and ^{3}He

K. S. Dhuga, B. L. Berman, W. J. Briscoe, R. W. Caress,* and S. K. Matthews†
Center for Nuclear Studies, Department of Physics, The George Washington University, Washington, D.C. 20052

D. B. Barlow,‡ B. M. K. Nefkens, C. Pillai,‡ and J. W. Price§
Department of Physics, University of California at Los Angeles, California 90024

S. J. Greene
Los Alamos National Laboratory, Los Alamos, New Mexico 87545

I. Slaus and I. Supek
Department of Physics, Institute Rudjer Boskovic, Zagreb, Croatia
(Received 10 May 1996)

We have measured differential cross sections for pion elastic scattering from ^{3}H and ^{3}He in the angular region near the minimum in the non-spin-flip amplitude. Data were acquired for incident pion energies of 180, 220, 256, and 295 MeV. Nuclear charge symmetry is investigated with the aid of several charge-symmetric ratios formed from combinations of measured cross sections. A particularly intriguing result is obtained from the superratio R, which is defined as

$$R=\frac{d\sigma(\pi^+{}^3\mathrm{H})d\sigma(\pi^-{}^3\mathrm{H})}{d\sigma(\pi^+{}^3\mathrm{He})d\sigma(\pi^-{}^3\mathrm{He})}.$$

R is found to be *greater* than unity at 180 MeV and significantly *smaller* than unity at 256 MeV, with the transition occurring at around 210 MeV. The charge-symmetry prediction for this ratio (after allowance for the Coulomb force) is one, and is independent of energy and angle. [S0556-2813(96)00112-4]

PACS number(s): 21.45.+v, 24.80.+y, 25.10.+s, 25.80.Dj

I. INTRODUCTION

Over the years ample evidence has been gathered demonstrating that electromagnetic interactions alone are not sufficient to explain the existence of a small but persistent charge-symmetry-breaking (CSB) amplitude in the nuclear force. Some of this early evidence came from studies of isospin-multiplet mass splitting, such as the binding energy difference between ^{3}H and ^{3}He, and the inequality of the nucleon-nucleon scattering lengths. On the theoretical front, at least on the nucleon level, much progress has been made in our conceptual understanding of CSB in terms of ρ-ω (and π-η) meson-mixing models [1–3]. Moreover, theoretical models now exist that attempt to treat CSB in the framework of the mass difference of the up and down quarks and the electromagnetic interactions between them [4–6]. However, at the nucleus level our understanding of CSB is less than satisfactory both from the experimental and theoretical viewpoints. For a review of the experimental and theoretical status of CSB in the nuclear force, the reader is referred to a recent article on the subject by Miller *et al.* [7].

In recent years, the study of pion elastic scattering from isospin-mirror nuclei, in particular $A=2$ [8–10] and $A=3$ [11–13], has provided further indications of CS violation. Primarily, these studies focused on the behavior of a number of charge-symmetric ratios determined from the measured elastic differential cross sections. Specifically, we reproduce here the ratios used in the $A=3$ studies. These include the cross-section ratios ρ^+, ρ^-, and the charge-symmetric ratios r_1, r_2, and R (the superratio):

$$\rho^+=\frac{d\sigma(\pi^+{}^3\mathrm{H})}{d\sigma(\pi^+{}^3\mathrm{He})}, \quad \rho^-=\frac{d\sigma(\pi^-{}^3\mathrm{H})}{d\sigma(\pi^-{}^3\mathrm{He})},$$

$$r_1=\frac{d\sigma(\pi^+{}^3\mathrm{H})}{d\sigma(\pi^-{}^3\mathrm{He})}, \quad r_2=\frac{d\sigma(\pi^-{}^3\mathrm{H})}{d\sigma(\pi^+{}^3\mathrm{He})},$$

$$R=\rho^+\rho^-=r_1r_2.$$

The systematic energy and angle behavior of the charge-symmetric ratios, and in particular the deviation of these ratios from the values predicted by CS (with allowance for the

*Present address: Burlington Engineering Labs, North Carolina State University, Raleigh, NC 27612.
†Present address: Physics Department, Catholic University of America, Washington, D.C. 20064.
‡Present address: Los Alamos National Laboratory, Los Alamos, NM 87545.
§Present address: Department of Physics, Rensselaer Polytechnic Institute, Troy, NY 12180.

Coulomb force) has been interpreted as an unambiguous indicator of a nonzero CSB amplitude in the scattering process.

The study of the isospin-mirror combinations $\pi^+ {}^3\mathrm{H}$ and $\pi^- {}^3\mathrm{He}$ (as well as $\pi^- {}^3\mathrm{H}$ and $\pi^+ {}^3\mathrm{He}$) in the Δ region, where the spin and isospin structure of the basic πN interaction is dominated by a single partial wave, provides an excellent opportunity for testing nuclear CS. Further, not only do accurate correlated three-body wave functions exist as input for realistic calculations, but all the isospin pairs are available for pion-scattering measurements as well. In principle, this makes it relatively straightforward to test nuclear CS by exploring systematic differences in the scattering from members of isospin pairs, provided that appropriate corrections are made for the effects of the Coulomb force.

In this work, we present the results of our pion-trinucleon elastic-scattering measurements (ratios and differential cross sections) at 180, 220, 256, and 295 MeV. One particular goal of these measurements was to investigate simultaneously (without the use of a polarized target) the nature of the relative roles of both the spin-flip (SF) and the non-spin-flip (NSF) amplitudes in the π-nucleus scattering system. Simple pion-trinucleon kinematics, coupled with the angular behavior of the basic πN scattering amplitudes, indicate that the optimum kinematic region for this study (given the above energy range) is around 75° (in the laboratory frame). Essentially, in this angular region, the SF amplitude happens not only to be near its maximum but also is comparable in magnitude to the rapidly changing NSF amplitude. We note that the largest CSB effect (for both $A=2$ and 3 nuclei) reported thus far is precisely in this angular region. Furthermore, the important role played by the SF amplitude in pion-trinucleon scattering, particularly in this (energy and) angular region, is amply demonstrated by recent studies [14,15] of pion elastic scattering on polarized ^{3}He, which report a large asymmetry—an asymmetry which is directly due to the interference of the π-nuclear spin-flip and non-spin-flip amplitudes.

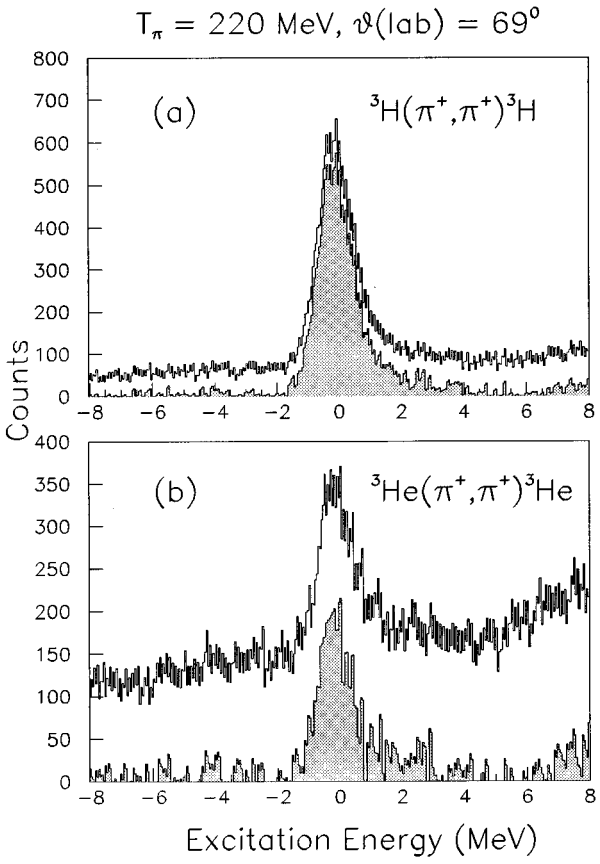

FIG. 1. Raw and background-subtracted excitation-energy spectra for $T_\pi = 220$ MeV and a laboratory angle of 69°. Note the large difference between the yields for $\pi^+ {}^3\mathrm{H}$ (a) and $\pi^+ {}^3\mathrm{He}$ (b) at this angle near the NSF dip.

II. EXPERIMENT

We have measured π^+ and π^- elastic scattering from ^{3}H and ^{3}He. The experiments were performed with the Energetic Pion Channel and Spectrometer (EPICS) [16] at the Los Alamos Meson Physics Facility (LAMPF). Data were acquired at incident pion energies of 180, 220, 256, and 295 MeV. The 256-MeV data include four angle settings (i.e., laboratory scattering angles of 50°, 66°, 75°, and 89°), whereas the remaining measurements were made at a single angle—the angle corresponding to the location of the NSF dip in pion elastic scattering from the $A=3$ nuclei.

Our targets consisted of high-pressure gases (^{3}H, ^{3}He, ^{2}H, and ^{1}H) sealed in cylindrical containers approximately 12.7 cm in diameter and 22.9 cm in length. The target cells had special aluminum walls with a small diffusion coefficient for hydrogen and a high tensile strength. Other details of the targets, experimental setup, and, in particular, procedures used to determine the number of atoms in each gas sample have been described previously [13,17].

The precise position of the NSF dip is not well known. However, it is well established that for the pion-nucleon case, this dip occurs at about 90° in the center-of-mass frame (for a range of energies centered around the peak of the Δ

TABLE I. $\pi^\pm$-trinucleon cross-section ratios in the angular region spanning the NSF dip.

T_π (MeV)	θ_{cm} (deg)	ρ^+	ρ^-	R
180	78.8	2.3 ± 0.1	0.50 ± 0.03	1.15 ± 0.09
220	75.3	3.5 ± 0.2	0.27 ± 0.02	0.95 ± 0.09
256	82.1	0.50 ± 0.04	1.4 ± 0.1	0.70 ± 0.08
295	80.6	0.10 ± 0.01	6 [a]	0.6 [a]

[a]Lower limit values.

TABLE II. Charge-symmetric ratios in the angular region spanning the NSF dip.

T_π (MeV)	θ_{cm} (deg)	r_1	r_2	R
180	78.8	0.99 ± 0.06	1.19 ± 0.08	1.2 ± 0.1
220	75.3	1.00 ± 0.08	0.93 ± 0.09	0.9 ± 0.1
256	82.1	1.0 ± 0.1	0.74 ± 0.08	0.7 ± 0.1
295	80.6	0.8 [a]	0.8 ± 0.2	0.6 [a]

[a]Lower limit values.

resonance). Due to kinematic transformations the location of this dip is expected to shift approximately to 75° (in the laboratory frame) for the pion-trinucleon case at the peak of the Δ resonance. Initial exploratory measurements of π^+ ^{3}He elastic scattering were made around the setting of 75° ($\pm 3°$) for incident pion energies of 180 and 256 MeV to locate the position of the dip. A minimum in the normalized elastic yield provided this location. Our previous measurements [13] at 220 MeV and those of Kallne *et al.* [18] at 295 MeV were used to determine the angular position of the dip for these other energies.

The data-taking sequence was as follows: for each scattering angle the spectrometer was tuned for π^+ elastic scattering from ^{3}H, and we measured, in turn, the yield from ^{3}H, ^{3}He, and ^{2}H. (The deuterium measurements were made for the purpose of background subtraction.) The spectrometer was next tuned for π^+ elastic scattering from ^{2}H, and we measured the yield from deuterium and hydrogen. These deuterium measurements (after appropriate background subtractions using the hydrogen data) provide the normalizations for the π^+ elastic-scattering cross sections for ^{3}H and ^{3}He. For a few cases, we next tuned the spectrometer for π^+ elastic scattering from hydrogen; these data serve as a doublecheck for our normalizations. After the π^+ measurements were completed for a given angle setting, the channel and spectrometer were next tuned for π^-, and the entire data-taking sequence was repeated without further changes to the experimental setup.

We used several beam monitors to measure the relative pion flux. These included a primary-beam toroidal current monitor (located upstream of the production target), a solid-state detector monitoring the reaction products from the primary production target, an ionization chamber in the EPICS scattering chamber, and a pair of thin plastic-scintillator ΔE-E telescopes located several meters downstream of the (gas) target, primarily to measure muons from in-flight pion decay. Throughout the experiment these monitors provided a very stable measurement of the relative pion flux, and in all cases, agreed with each other to better than 2%. In order to remove protons from the incident pion flux, a thick (0.25″) graphite degrader was inserted in the pion channel. To maintain similar conditions for the π^+ and π^- beams, the same degrader was used for the π^- measurements. (The electron contamination of the pion beam was not directly monitored; it is known to be small [19].)

III. DATA REDUCTION AND RESULTS

Using two-body kinematics and momentum and position information for each scattered event as measured with the spectrometer and wire-chamber detector package of the EPICS system, excitation-energy histograms were obtained. Since the EPICS system enables one to reconstruct particle trajectories back to the target position, one can use software cuts on histograms of various target projections to remove scattering contributions from the target walls and support flanges. By this technique, an optimum set of software cuts was arrived at by maximizing the signal-to-background ratio for each spectrometer setting. The same optimum cuts were used to replay the entire set of π^+ and π^- data. Displayed in Fig. 1 are typical excitation-energy spectra showing both the raw and the background-subtracted yields for π^+ on ^{3}H [Fig. 1(a)] and π^+ on ^{3}He [Fig. 1(b)] for 220 MeV and 69° laboratory angle.

The normalized elastic yield from each target is obtained from the number of counts in the elastic peak of the excitation-energy spectrum and a normalization factor which is dependent on several variables, including wire-chamber efficiencies, the survival factor for the scattered pions in the spectrometer, the flux measurement by one of the beam monitors, and the computer live time. For the extraction of ratios of relative cross sections (defined below), the summing range of the elastic peak was from -1 to $+1$ MeV. However, in order to include the total area under the peak for the elastic cross sections, it was necessary to extend the summing range from -2 to $+2.5$ MeV (see Fig. 1). We express the relative cross-section ratios (ρ^+, ρ^-) and the charge-symmetric ratios (r_1, r_2) in terms of the measured yields:

$$\rho^+ = \frac{[Y(\pi^+\,{}^3\mathrm{H}) - Y(\pi^+_{\mathrm{bk}})]}{[Y(\pi^+\,{}^3\mathrm{He}) - Y(\pi^+_{\mathrm{bk}})]} \cdot \frac{N(^3\mathrm{He})}{N(^3\mathrm{H})},$$

$$\rho^- = \frac{[Y(\pi^-\,{}^3\mathrm{H}) - Y(\pi^-_{\mathrm{bk}})]}{[Y(\pi^-\,{}^3\mathrm{He}) - Y(\pi^-_{\mathrm{bk}})]} \cdot \frac{N(^3\mathrm{He})}{N(^3\mathrm{H})},$$

$$r_1 = \frac{[Y(\pi^+\,{}^3\mathrm{H}) - Y(\pi^+_{\mathrm{bk}})]}{[Y(\pi^-\,{}^3\mathrm{He}) - Y(\pi^-_{\mathrm{bk}})]} \cdot \frac{[Y(\pi^-\,{}^2\mathrm{H}) - Y(\pi^-_{\mathrm{bk}})]}{[Y(\pi^+\,{}^2\mathrm{H}) - Y(\pi^+_{\mathrm{bk}})]} \cdot \frac{N(^3\mathrm{He})}{N(^3\mathrm{H})},$$

$$r_2 = \frac{[Y(\pi^-{}^3\mathrm{H}) - Y(\pi^-_{\mathrm{bk}})]}{[Y(\pi^+{}^3\mathrm{He}) - Y(\pi^+_{\mathrm{bk}})]} \cdot \frac{[Y(\pi^+{}^2\mathrm{H}) - Y(\pi^+_{\mathrm{bk}})]}{[Y(\pi^-{}^2\mathrm{H}) - Y(\pi^-_{\mathrm{bk}})]} \cdot \frac{N(^3\mathrm{He})}{N(^3\mathrm{H})},$$

TABLE III. $\pi^{\pm}$-trinucleon cross-section ratios for 256-MeV incident pion energy.

θ_{cm} (deg)	ρ^+	ρ^-	R
55.7	0.91 ± 0.04	1.08 ± 0.05	0.98 ± 0.06
72.7	1.06 ± 0.06	0.71 ± 0.05	0.75 ± 0.07
82.1	0.50 ± 0.04	1.4 ± 0.1	0.70 ± 0.08
96.2	0.82 ± 0.08	1.3 ± 0.2	1.1 ± 0.2

TABLE IV. Charge-symmetric ratios for 256-MeV incident pion energy.

θ_{cm} (deg)	r_1	r_2	R
55.7	0.97 ± 0.05	1.02 ± 0.05	0.99 ± 0.07
72.7	1.1 ± 0.1	0.72 ± 0.06	0.8 ± 0.1
82.1	1.0 ± 0.1	0.74 ± 0.08	0.7 ± 0.1
96.2	1.2 ± 0.3	0.9 ± 0.2	1.1 ± 0.4

where $Y(\pi^{\pm}A)$ is the $\pi^{\pm}$ elastic yield for $A={}^3$H, ^{3}He, or ^{2}H; $Y(\pi^{+-}_{bk})$ is the background yield, and $N(^3\mathrm{H})$ and $N(^3\mathrm{He})$ are the number of atoms in the tritium and helium targets, respectively. As noted in the previous section, the deuterium target cell (with kinematics set for pion elastic scattering from ^{3}H) was used to obtain the background yields for the $A=3$ measurements. Likewise, the hydrogen target (with kinematics set for pion elastic scattering from ^{2}H was used to measure the background for the deuterium yields. Furthermore, in the expressions for the ratios r_1 and r_2 we have assumed that $d\sigma(\theta)[\pi^{+}\,{}^2\mathrm{H}]=d\sigma(\theta)[\pi^{-}\,{}^2\mathrm{H}]$. Measurements [20,21] indicate this to be a very good approximation (for the energies and angles of this experiment).

As noted in earlier work [12,13,17], the ratios ρ^+ and ρ^- are independent of the absolute beam normalization, the detector efficiency, and solid angle. This is because the same pion polarity appears in both the numerator and the denominator and hence the various flux- and detector-related normalizations cancel. This simplicity provides an elegant method for the extraction of the superratio with minimum systematic uncertainty. However, this is not the case for the ratios r_1 and r_2, which involve opposite pion polarities. In these ratios, we note the appearance of the deuterium normalization yields. The extra step involving the measurement of deuterium yields leads to an additional uncertainty in the value extracted for R from these ratios.

From the measured yields, we also determine the π^+ and π^- elastic-scattering differential cross sections for ^{3}H and ^{3}He. The measured (π^+ and π^-) deuterium yields together with published $\pi^{\pm}\,{}^2$H cross-section data [20,21] provide the normalizations for the differential cross sections.

The numerical results for the ratios ρ^+, ρ^-, and the superratio R (in the angular region of the NSF dip) for 180, 220, 256, and 295 MeV incident pion energies are listed in Table I. The momentum-transfer range covered by these measurements extends from 1.7 to 2.4 fm^{-1}. Listed in Table II are the charge-symmetric ratios r_1 and r_2 (along with R). In Tables III–V, we summarize the angular-distribution data as well as the ratios r_1, r_2, and the superratio R for 256-MeV incident pion energy. Finally, in Table VI, we provide the pion-trinucleon elastic-scattering differential cross sections (at the angle corresponding to the location of the NSF dip) for incident pion energies of 180, 220, and 295 MeV. In the case of the 295-MeV points only an upper limit was established for the π^--^{3}He yield. Results obtained from this yield are identified in the tables as lower or upper limits. The quoted uncertainties reflect the statistical uncertainties in the extraction of yields as well a 3% systematic uncertainty (folded in quadrature) due to background subtraction procedures (described in detail in Refs. [13,17]).

IV. DISCUSSION OF RESULTS AND CALCULATIONS

A. Experimental results

We note that the ratios ρ^+ and ρ^- differ substantially from unity and from each other; this is not a surprising result since these ratios are not constrained by CS. Instead, these ratios reflect the underlying energy and angle behavior of the πN spin-flip (SF) and non-spin-flip (NSF) scattering amplitudes. It is well established that forward-angle differential cross sections for π-nucleus elastic scattering is dominated by the NSF amplitude. In the angular region near the NSF dip, however, the SF amplitude makes a sizable contribution to the scattering, and thus must be included in any description of the ρ^+ and ρ^- ratios. Furthermore, contributions due to the SF amplitude are expected to produce opposite trends in these ratios. We illustrate this point by noting that for on-resonance pions [for which $\sigma(\pi^+p)$ is $\approx 9\sigma(\pi^+n)$] the numerator in ρ^+ (i.e., $\pi^+\,{}^3$H) is dominated by π^+p scattering. Both SF and NSF amplitudes contribute to the scattering. In the denominator the scattering is mainly from the spin-paired protons in ^{3}He. For this case the simple argument suggests that only NSF scattering is possible because the contribution from the SF amplitude is forbidden by the Pauli principle. When applied to the region of the NSF dip, this argument predicts a maximum for the ρ^+ ratio because of the vanishing NSF amplitude in the denominator. Likewise, the same simple picture predicts a corresponding minimum in the ρ^- ratio. Despite the fact that this simple picture is nearly valid for resonance-energy pions only, the rapidly

TABLE V. $\pi^{\pm}$-trinucleon elastic-scattering differential cross sections at 256 MeV.

θ_{cm} (deg)	$\pi^+\,{}^3$H (mb/sr)	$\pi^-\,{}^3$H (mb/sr)	$\pi^+\,{}^3$He (mb/sr)	$\pi^-\,{}^3$He (mb/sr)
55.7	1.6 ± 0.1	1.8 ± 0.1	1.7 ± 0.1	1.7 ± 0.1
72.7	0.12 ± 0.01	0.081 ± 0.008	0.12 ± 0.02	0.12 ± 0.01
82.1	0.038 ± 0.005	0.055 ± 0.007	0.08 ± 0.01	0.041 ± 0.007
96.2	0.031 ± 0.003	0.034 ± 0.004	0.037 ± 0.004	0.025 ± 0.004

TABLE VI. $\pi^{\pm}$-trinucleon elastic-scattering differential cross sections at other energies.

T_π (MeV)	θ_{cm} (deg)	π^+ ^{3}H (mb/sr)	π^- ^{3}H (mb/sr)	π^+ ^{3}He (mb/sr)	π^- ^{3}He (mb/sr)
180	78.8	0.60 ± 0.04	0.30 ± 0.03	0.26 ± 0.03	0.59 ± 0.05
220	75.3	0.20 ± 0.03	0.051 ± 0.008	0.056 ± 0.009	0.19 ± 0.03
295	80.6	0.007 ± 0.001	0.055 ± 0.008	0.072 ± 0.007	0.009 [a]

[a]Upper limit value.

angle-dependent and oscillatory features predicted for ρ^+ and ρ^- show up prominently both in resonance and off-resonance data. Although the angular behavior of these ratios can be understood qualitatively from the known angular dependence of the πN scattering amplitudes (for a given momentum transfer), the absolute magnitudes of these ratios, however, are not so simply interpreted. This is especially true for the data in the NSF-dip region where (because the first-order contributions to the scattering are small) higher-order contributions, including effects due to multiple scattering, cannot be neglected. In essence, there is no simple factorization between effects due to a dominant reaction mechanism and those due to the details of the nuclear structure.

From the perspective of isospin invariance, the more significant deviation is that of the superratio R, for which CS would predict a value of unity, provided the effects of the Coulomb force are taken into account. The superratio clearly deviates from unity (see Tables I and II). Furthermore, we note that in the NSF dip, R is *greater* than unity at 180 MeV and is significantly *smaller* than unity at 256 MeV. At 220 MeV, on the other hand, R is consistent with one. The measurements at 295 MeV, despite being hampered by very small cross sections, especially for π^- ^{3}He (hence the lower limit quote for R), also indicate a much smaller value for R. It would appear from these data that in the vicinity of the NSF dip, the superratio undergoes a transition, from values greater than unity to those smaller than unity as a function of energy across the Δ-resonance region, with the transition occurring at around 210 MeV. This transitional behavior of the superratio is seen clearly in Fig. 2, which shows a plot of R as a function of the incident pion energy. In this plot, we have included data from one of our earlier measurements [13] at 142 MeV. Even with the poor statistics for the point at 295 MeV (indicated by an arrow denoting a lower limit), the downward trend of the superratio as a function of incident pion energy is clearly evident. Incidentally, we note that in this same energy range a similar transitional behavior seems to be exhibited by the asymmetry for pion elastic scattering from polarized ^{3}He [15].

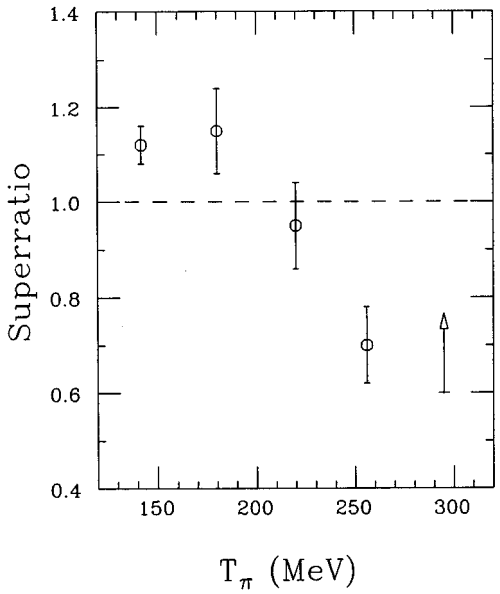

FIG. 2. The superratio R (in the NSF-dip region), showing clearly the transition from values greater than one to those smaller than one with increasing incident pion energy. The arrow on the 295-MeV datum is used to denote a lower limit.

The individual charge-symmetric ratios r_1 and r_2 are also determined by CS and should be equal to unity as functions of energy and angle. This is certainly the case for r_1, which is clearly consistent with unity across the NSF dip. However, the situation is dramatically different for r_2; it deviates significantly from the CS value, and is the origin of the observed greater-than-one value for R at 180 MeV and the less-than-one value at 256 MeV. In Fig. 3, we display the angular behavior of the charge-symmetric ratios for 256 MeV; the data clearly indicate that it is the magnitude and the angular dependence of the ratio r_2 that is primarily responsible for the observed variation in the superratio R.

B. Comparison with theory

In the recent past, several theoretical model calculations [22–24] (based on the multiple-scattering series and the impulse approximation) have appeared in the literature that attempt to explain the behavior of our earlier data, particularly that of the superratio at 180 MeV. For example, the main thrust of the argument advanced by Kim *et al.* [22] is that the Coulomb interaction distorts the nuclear force sufficiently (via the interference of Coulomb and nuclear amplitudes resulting in a change in the purely nuclear phase) to cause the observed deviation of R. Apart from the Coulomb distortions, the main ingredients in their momentum-space optical-model calculation include the experimental charge and magnetic form factors of the three-body nuclei and a second-order term proportional to ρ^2, the square of the nucleon density. Although the effect due to the Coulomb repulsion between the two protons in ^{3}He (which leads to a structural difference between the ^{3}He and ^{3}H nuclei [25]) is not explicitly included, some compensation for this effect is achieved implicitly through the use of the experimental charge form factors. The second-order term (the details of which are not specified) is presumably needed to account for

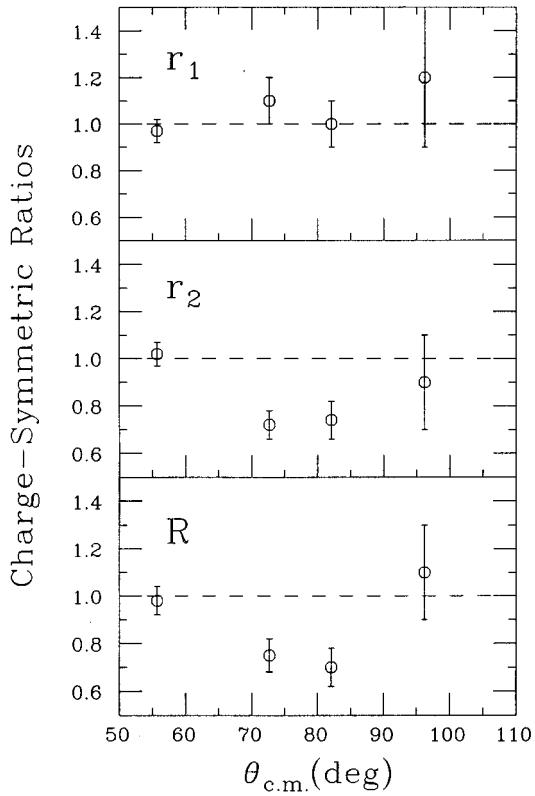

FIG. 3. Charge-symmetric ratios for 256-MeV incident pion energy. Note that the magnitude of the superratio R near the NSF dip is significantly smaller than unity, and its shape is determined primarily by the angular dependence of r_2.

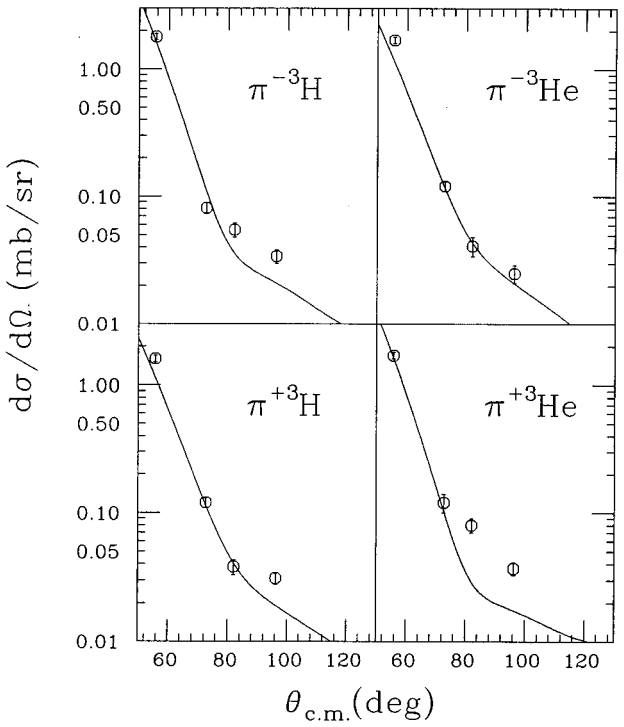

FIG. 4. Differential cross sections for pion-trinucleon elastic scattering at 256 MeV. The solid curve is the result of a momentum-space optical-model calculation [23] that employs correlated three-body wave functions.

higher-order inelastic-scattering effects not directly included in the standard multiple-scattering series, as well as effects due to true pion absorption—a channel which is not only known to be important in this energy region but also one that exhibits a dramatic isospin dependence [26–28]. Another important issue raised by their analysis (but not discussed, however) is whether it is appropriate, in pion-nucleon scattering calculations, to use as input electromagnetic form factors determined directly from electron-scattering data with the usual attendant uncertainties concerning the role of exchange currents. As has been known for a long time [29–31], this is particularly worrisome in the case of trinucleon magnetic form factors, where the corrections due to meson-exchange currents (even at moderate momentum transfer) are predicted to be large and model dependent.

Kamalov *et al.* [23] also construct an optical potential (in momentum space) to describe pion-elastic cross sections for light-to-heavy nuclei. We show in Fig. 4 our differential cross sections for pion-trinucleon elastic scattering at 256 MeV, along with the results of Ref. [23]. The forward-angle behavior of the cross sections is well reproduced. However, significant discrepancy between data and theory exists in the angular region which is nominally dominated by the SF amplitude. In this calculation, these authors avoid the ambiguities related to the use of electromagnetic form factors by employing correlated three-body wave functions obtained from the solution of the Faddeev equations (solved with the use of the Reid potential for the NN interaction). Further, in constructing the first-order potential, Kamalov *et al.* do not use the usual ''$t\rho$ factorization'' approximation [32] (where t is the πN t matrix and ρ is the nucleon density); instead the full integral is evaluated exactly. However, these authors, too, found it necessary to employ a phenomenological second-order scalar term in their potential to obtain reasonable agreement with pion elastic-scattering data for medium-to-heavy nuclei. For their pion-trinucleon calculations, they note that their ρ^2 scalar term is, at best, a crude approximation. Furthermore, the ρ^2 term does not have the necessary spin and isospin structure. An added uncertainty arises because this phenomenological term is known to exhibit an energy dependence, the nature of which is not entirely understood.

Surprisingly, although both Kamalov *et al.* and Kim *et al.* obtain similar results for the 180-MeV differential cross sections (and in good agreement with the data in the forward-angle region), their results for the superratio are strikingly different. In fact, Kamalov *et al.* predict the superratio to be *less* than one at 180 MeV and *greater* than one at 220 MeV, in complete contrast to the data. Despite disagreeing markedly in these predictions for the superratio, the authors are apparently in agreement as to the cause of the observed behavior, namely Coulomb-nuclear interference.

A calculation that leads to a quite different conclusion concerning the role of the Coulomb force was reported by Gibbs and Gibson [24]. In this calculation, the authors employ an optical potential in configuration space, and use as input neutron and proton densities generated from wave functions obtained from three-body Faddeev calculations. Nominally, the neutrons and protons are expected to have similar distributions. In fact, an argument based on CS would

predict identical distributions for the proton in ^{3}H and the neutron in ^{3}He. In the absence of the Coulomb force between the protons in ^{3}He, a similar statement would apply to the protons in ^{3}He and the neutrons in ^{3}H. Allowing for structural differences between these nuclei, Gibbs and Gibson rescaled the particle densities to fit the pion-trinucleon cross-section data at 180 MeV, and as a result of this fitting procedure (which involves varying the difference between the even-nucleon and odd-nucleon radii), they were able to achieve a good description of the superratio. They also found that the superratio was little affected by any of the many parameters and model assumptions of the πN-scattering calculation; by far the largest effect was due to the difference in the proton and neutron radii. The fitting procedure produced radius differences (for the odd- and even-nucleon cases) that were consistent with those determined by Faddeev calculations that explicitly included CSB via ρ-ω mixing. From these results, Gibbs and Gibson concluded that the magnitude and the angular behavior of the charge-symmetric ratios, particularly that of the superratio R, was indicative of a significant CSB effect above and beyond that would be expected from the Coulomb interaction alone. A similar analysis of our 256-MeV data is underway [33].

V. SUMMARY AND CONCLUSIONS

For several incident pion energies—180, 220, 256, and 295 MeV—we have obtained differential cross-section data, spanning the NSF dip, for the scattering of the pion-trinucleon isospin pairs (π^+ ^{3}H and π^- ^{3}He) and (π^- ^{3}H and π^+ ^{3}He). The charge-symmetric ratios formed from the cross sections for these isospin pairs provide a measure of CS violation in the πN and πA systems. The superratio R is found to vary significantly from its CS value; in particular, it exhibits a transition in behavior as a function of incident pion energy: it is *greater* than unity at 180 MeV and *smaller* than unity at 256 MeV, with the transition occurring at approximately 210 MeV. Reproduction of this feature alone constitutes a major challenge to all current pion-nuclear scattering theories. Another observation that these models must explain is the fact that the angular behavior of the superratio at 256 MeV is determined largely by the angular distribution of the ratio r_2; the ratio r_1 is quite clearly consistent with its CS value (of one) throughout the NSF-dip region. This feature is also observed in the NSF dip for pion energies of 142 and 180 MeV.

Although several theoretical models are able to achieve reasonably good descriptions for the individual forward-angle differential cross sections at 180 MeV (and higher energies), none, so far, even with the aid of sophisticated three-body wave functions, has quantitatively reproduced the energy and angle behavior of the superratio without the explicit introduction of a CSB amplitude above and beyond that due to the Coulomb force. Interestingly, two models ([22,23]) that lead to very similar results for the pion-trinucleon cross sections at 180 MeV produce strikingly different values for the superratio. What makes this result unusual is the fact that in both models the same physical process, i.e., Coulomb-nuclear interference, is cited as the primary cause for the deviation of the superratio from its CS value. Clearly, the proper inclusion of the effects of the Coulomb force in the calculation of the π-nucleus t matrix is not a trivial matter. Indeed, theoretical complications arising from Coulomb corrections have been noted before [9], in the analysis of the $\pi^\pm$ ^{2}H differential cross sections.

Moreover, it is now generally accepted that a good description of these small pion-trinucleon cross sections, particularly in the very sensitive region of the NSF dip, can only come about if higher-order effects such as those due to inelastic scattering and true pion absorption are included, with full preservation of the spin and isospin structure of the basic πN interaction. In this respect, the energy and angle dependence of the relative cross-section ratios ρ^+ and ρ^- may prove to be useful in gauging the sensitivity of the input parameters describing the underlying scattering theory.

ACKNOWLEDGMENTS

We thank J. Van Dyke, H. R. Maltrud, and L. L. Sturgess for their expert technical help and D. A. Hanson and C. E. Smith for their help during the data-acquisition stage of the experiment. This work was supported in part by the U.S. Department of Energy and the National Science Foundation under Grants DE-FG05-86ER40285, DE-FG05-86-ER40270, PHY-8907284, and PHY-9122139, respectively.

[1] S.A. Coon and R.C. Barret, Phys. Rev. C **36**, 2189 (1987).
[2] L.N. Epele, H. Fanchiotti, C.A. Garcia Canal, and R. Mendez Galain, Phys. Rev. D **39**, 1473 (1989).
[3] G.A. Miller, Nucl. Phys. **A518**, 345 (1990), and references therein.
[4] P. Langacker, Phys. Rev. D **20**, 2983 (1979).
[5] G. Krein, A.W. Thomas, and A.G. Williams, Phys. Lett. B **317**, 293 (1993).
[6] K.L. Mitchell, P.C. Tandy, C.D. Roberts, and R.T. Cahill, Phys. Lett. B **335**, 282 (1994).
[7] G.A. Miller, B.M.K. Nefkens, and I. Slaus, Phys. Rep. **194**, 1 (1990).
[8] E. Pedroni, K. Gabathuler, J.J. Domingo, W. Hirt, P. Schwaller, J. Arvieux, C.H.Q. Ingram, P. Gretillat, J. Piffaretti, N.W. Tanner, and C. Wilkin, Nucl. Phys. **A300**, 321 (1978).
[9] T.G. Masterson, E.F. Gibson, J.J. Kraushaar, R.J. Peterson, R.S. Raymond, R.A. Ristinen, and R.L. Boudrie, Phys. Rev. Lett. **47**, 220 (1981); T.G. Masterson, J.J. Kraushaar, R.J. Peterson, R.S. Raymond, R.A. Ristinen, J.L. Ullmann, R.L. Boudrie, D.R. Gill, E.F. Gibson, and A.W. Thomas, Phys. Rev. C **30**, 2010 (1984).
[10] G.R. Smith, D.R. Gill, D. Ottewell, G.D. Wait, P. Walden, R.R. Johnson, R. Olszewski, R. Rui, M.E. Sevior, R.P. Trelle, E.L. Mathie, V. Pafilis, J. Brack, J.J. Kraushaar, R.A. Ristinen, H. Chase, R.B. Schubank, N.R. Stevenson, A. Rinat, and Y. Alexander, Phys. Rev. C **38**, 240 (1988).
[11] B.M.K. Nefkens, W.J. Briscoe, A.D. Eichon, D.H. Fitzgerald, J.A. Holt, A. Mokhtari, J.A. Wightman, M.E. Sadler, R.L.

Boudrie, and C.L. Morris, Phys. Rev. Lett. **52**, 735 (1984); C. Pillai, D.B. Barlow, B.L. Berman, W.J. Briscoe, A. Mokhtari, B.M.K. Nefkens, A.M. Petrov, and M.E. Sadler, Phys. Lett. B **207**, 389 (1988).

[12] B.M.K. Nefkens, W.J. Briscoe, A.D. Eichon, D.H. Fitzgerald, A. Mokhtari, J.A. Wightman, and M.E. Sadler, Phys. Rev. C **41**, 2770 (1990).

[13] C. Pillai, D.B. Barlow, B.L. Berman, W.J. Briscoe, A. Mokhtari, B.M.K. Nefkens, and M.E. Sadler, Phys. Rev. C **43**, 1838 (1991).

[14] B. Larson, O. Hausser, E.J. Brash, C. Chen, A. Rahav, C. Bennhold, P.P.J. Delheij, R.S. Henderson, B.K. Jennings, A. Mellinger, D. Ottewell, A. Trudel, S. Ram, L. Tiator, and S.S. Kamalov, Phys. Rev. Lett. **67**, 3356 (1991).

[15] M. Espy, D. Dehnhard, C. Edwards, M. Palarczyk, J. Langenbrunner, B. Davis, G.R. Burleson, S. Blanchard, W.R. Gibbs, B. Lail, B. Nelson, B.K. Park, Q. Zhao, W. Cummings, P.P.J. Delheij, B.K. Jennings, R. Henderson, O. Hausser, D. Thiessen, E. Brash, M.K. Jones, B. Larson, B. Brinkmoller, K. Maeda, C.L. Morris, J.M. O'Donnell, S. Penttila, D. Swenson, D. Tupa, C. Bennhold, and S.S. Kamalov, Phys. Rev. Lett. **76**, 3667 (1996).

[16] H.A. Thiessen, Los Alamos Internal Report LA-6663-MS, 1977 (unpublished); R.L. Boudrie, J.F. Amman, C.L. Morris, H.A. Thiessen, and L.E. Smith, IEEE Trans. Nucl. Sci. **NS26**, 4588 (1979); J.F. Amman, R.L. Boudrie, H.A. Thiessen, C.L. Morris, and L.E. Smith, *ibid*. **NS26**, 4389 (1979); L.G. Atencio, J.F. Amman, R.L. Boudrie, and C.L. Morris, Nucl. Instrum. Methods **187**, 381 (1981).

[17] S.K. Matthews, Ph.D. thesis, The George Washington University, 1993 (unpublished).

[18] J. Kallne, J.F. Davis, J.S. McCarthy, R.C. Minehart, R.R. Whitney, R.L. Boudrie, J. McClelland, and A. Stetz, Phys. Rev. Lett. **45**, 517 (1980).

[19] K.G. Boyer, Los Alamos National Laboratory Report LA-9974-T, 1984 (unpublished).

[20] K. Gabathuler, J. Domingo, P. Gram, W. Hirt, G. Jones, P. Schwaller, J. Zichy, J. Bolger, Q. Ingram, J.P. Albanese, and J.R. Arvieux, Nucl. Phys. **A350**, 253 (1980).

[21] C.R. Otterman, E.T. Boschitz, W. Gyles, W. List, R. Tacik, R.R. Johnson, G.R. Smith, and E.L. Mathie, Phys. Rev. C **32**, 928 (1985).

[22] K.Y. Kim, Y.E. Kim, and R.H. Landau, Phys. Rev. C **36**, 2155 (1987).

[23] S.S. Kamalov, L. Tiator, and C. Bennhold, Phys. Rev. C **47**, 941 (1993).

[24] W.R. Gibbs and B.F. Gibson, Phys. Rev. C **43**, 1012 (1991).

[25] J.L. Friar, B.F. Gibson, and G.L. Payne, Phys. Rev. C **35**, 1502 (1987).

[26] D. Ashery, R.J. Holt, H.E. Jackson, J.P. Schiffer, J.R. Specht, K.E. Stephenson, R.D. McKeown, J. Unger, R.E. Segel, and P. Zupranski, Phys. Rev. Lett. **47**, 895 (1981).

[27] T.S.H. Lee and K. Ohta, Phys. Rev. Lett. **49**, 1079 (1982).

[28] K.B. Yoo and R.H. Landau, Phys. Rev. C **25**, 489 (1982).

[29] A. Barroso and E. Hadjimichael, Nucl. Phys. **A238**, 422 (1975).

[30] I.V. Falomkin, V.I. Lyashenko, R. Mach, V.A. Panyushkin, G.B. Pontecorvo, M.G. Sapozhnikov, Yu. A. Shcherbakov, F. Balestra, M.P. Bussa, L. Busso, R. Garfagnini, T. Angelescu, I. Doniciu, M. Gavrilas, A. Mihul, F. Nichitiu, L. Pascu, and M. Antonova, Nuovo Cimento **57**, 111 (1980).

[31] E. Hadjimichael, Phys. Lett. B **172**, 156 (1985).

[32] R.H. Landau, Ann. Phys. **92**, 205 (1975); R.H. Landau and A.W. Thomas, Nucl. Phys. **A302**, 461 (1977).

[33] B.F. Gibson (private communication).